Fatma Nur Parın*, Kenan Yıldırım**

Preparation and Characterisation of Vitamin-Loaded Electrospun Nanofibres as Promising Transdermal Patches

DOI: 10.5604/01.3001.0014.3148

**Bursa Technical University,
Department of Polymer Materials Engineering,**
16310 Bursa, Turkey,
* e-mail: nur.parin@btu.edu.tr,
** e-mail: kenan.yildirim@btu.edu.tr

Abstract
In this study, bioactive fibres were produced using polyvinyl alcohol (PVA), gelatin, polyvinyl pyrrolidone (PVP) as a polymer matrix, and different amounts of folic acid (FA) as a vitamin using the electrospinning technique. Loading of the folic acid in the polymers was determined by Attenuated Total Reflectance-Fourier Transform Infrared Spectroscopy (ATR-FTIR); morphologies and average diameters were analysed by Scanning Electron Microscopy (SEM), and Thermal Gravimetric Analysis (TGA) was applied to determine thermal behaviours. The FTIR spectra and TGA thermograms showed the successful incorporation of folic acid into the fibres. SEM images showed that various smooth and heterogenous electrospun fibres were produced with average diameters ranging from 125 to 980 nm. An in-vitro study was carried out using dissolved FA in an artificial sweat solution (acidic media, pH 5.44), and UV-Vis analysis of electrospun fibres was made. The in vitro release study showed that the FA loaded nanofibres had initial vitamin burst release behaviour. The maximum vitamin release percentage of the PVA/FA, gelatin/FA, and PVP/FA fibres was obtained as 86.88%, 80.2%, and 76.66%, respectively. From these results, we can state that FA-loaded fibres can be potential candidates for transdermal patches and topical applications.

Key words: *vitamin release, folic acid, nanofibre, in-vitro study, electrospinning.*

Introduction

Nanofibres are an exciting new class of material which have a < 1 μm diameter and exhibit superior properties, such as a high surface area/volume ratio, low density, highly porous structure, and small pore size compared to conventional fibres [1-3]. Although there are various nanofibre fabrication techniques, such as melt blowing [4], melt electrospinning [5, 6], an island in the sea [7], phase separation [8], self-assembly [9, 10], and interface polymerisation [11], electrospinning is a cutting-edge technology which is preferred as a more promising approach for the fabrication of nanofibres. This technique has been used for almost 80 years due to its simplicity, versatility, cost-effectiveness, and ability to scale up. A wide range of syntheti, and natural polymers with nanoscale diameters were obtained [12-14]. These advantages of the technique enable large scale production for tissue engineering, biomedical, personal care (cosmetic), and drug delivery applications. In recent years, many studies have been conducted on the encapsulation of active agents (drug, vitamin, herbal extracts, and DNA) in electrospun fibres for skin tissue scaffolds [15-17], wound dressings [18, 19], dermal patches [20-22], and especially cosmeceutical products [23, 24].

Transdermal drug delivery systems (TDDS) refer to the administration of a therapeutic agent on the skin that is transported into the systemic circulation at a predetermined and precisely controlled rate to secure the patient [25, 26]. In this context, electrospun fibres can also be used as transdermal patches, and also they offer some advantages, such as site-specific drug delivery, enhanced therapeutic efficacy, and relatively low toxicity in comparison with oral delivery systems [27]. Besides this, encapsulating a drug in the fibre may protect the drug from external factors.

Vitamins are bioactive compounds that form a mixed chemical group. They assist the human immune system, promote skin health, and help cell growth. Unfortunately, vitamins are composed of molecules sensitive to light, heat, humidity, and pH conditions [28, 29]. If they are exposed to the above-mentioned conditions, they can be easily affected. Therefore, vitamins must be encapsulated for long-term uses.

Vitamin B_9 is an important member of the B-complex group and is also known as folic acid [30, 31]. Vitamin B_9 plays an essential role as a coenzyme for the maintenance of many metabolic functional processes in the body, such as cell growth and development, nucleic acid synthesis, and the metabolism of many amino acids [31, 32]. However, it is less stable than retinol, thiamine, riboflavin, and niacin, and it is more susceptible to both light and pH conditions as well [28]. Consequently, folic acid is applied in encapsulated forms for biological, nutriceutical, and pharmaceutical purposes.

During recent years, more attention has been paid and many attempts made to fabricate vitamin-loaded nanofibres in transdermal applications-drug delivery strategies. Azarbayjani *et al.* produced an anti-wrinkle nanofibre mask consisting of retinoic acid, ascorbic acid, gold nanoparticles, and collagen [23]. It was found that fibre mats can be an alternative to commercially available cotton face masks. Sheng *et al*. observed silk fibroin mats loaded with vitamin E as a potential candidate for skin renewal and care, as well as for tissue engineering applications [24]. In another study, Taepaiboon *et al.* compared the release amounts of cellulose acetate (CA) nanofibre mats and CA cast films containing vitamin A and E [33]. Besides this, the dermal therapeutic effects of the nanofibre were examined. Vitamin B_{12} is the most chemically complex molecule among of B group vitamins. It cooperates with vitamin B_9 in the formation of red blood cells. Therefore, PCL nanofibre loaded with vitamin B_{12} was produced

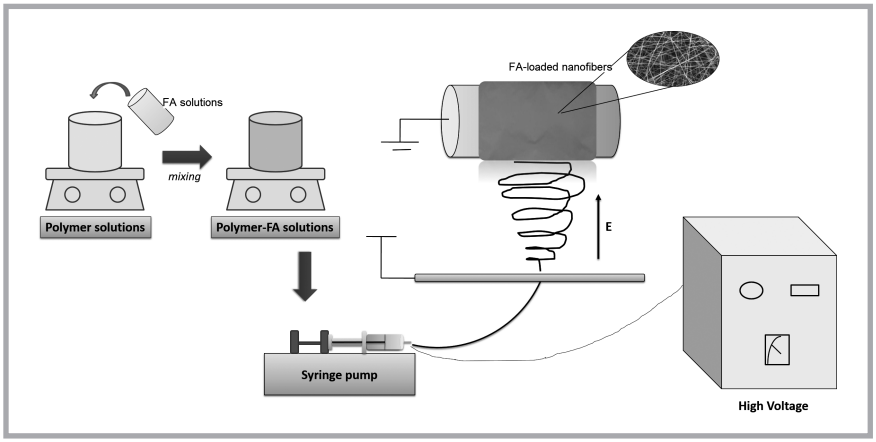

Figure 1. *Schematic illustration of electrospinning process.*

Table 1. *Materials used in the nanofibre fabrication.*

Chemicals	Property/codes	Manufacturer
PVA	Density 0.4-0.6 g/cm^3, purity 87.8%	ZAG Industrial Chemicals (Istanbul, Turkey)
PVP	K-30 (PVP, K-30)	Veskim Chemical Materials Co., Ltd. (Istanbul, Turkey)
Gelatin	Bovine skin (225 Bloom, type B)	Sigma Aldrich Chemical Company (USA)
Sodium bicarbonate ($NaHCO_3$)	99.7% purity	Sigma Aldrich Chemical Company (USA)
Acetic acid (CH_3COOH)	80% purity	Acros Organics Chemical Company (Belgium)
Ethanol	99.9% purity	Tekkim Chemical Company (Turkey)
Folic acid ($C_{19}H_{19}N_7O_6$)	98-102% purity, Biochemistry	ChemSolute Company (Germany)
Artificial sweat solutions ***(Figure 2)***	L-Histidine monohydrochloride monohydrate ($C_6H_9O_2N_3{\cdot}HCl{\cdot}H_2O$) (> 99% purity)	Sigma Aldrich Chemical Company (USA)
	Sodium chloride (> 99.5% purity)	
	sodium dihydrogen phosphate dihydrate ($NaH_2PO_4{\cdot}2H_2O$)	

for use in transdermal patch applications, and vitamin release behaviour was determined lasting up to 48 hours [34]. In a similar study, Li *et al.* successfully incorporated vitamin A and E into gelatin nanofibres for wound dressing application [35]. Moreover, thanks to the increment of collagen deposition in the wound repair of these vitamins, it was found that thr vitamin release behaviour of the nanofibres exhibit more than 60 hours of wound healing performance, which is better than commercial antiseptic products. Cosmetic and drug delivery are closely related areas. Electrospun nanofibres made of silk fibroin loaded with vitamin C were also investigated as skin regeneration applications, such as wound dressing and anti-ageing materials [36]. The wound healing property of electrospun CMCS/PEO nanofibres containing PHT-Na, and vitamin C were proved to be superior [37].

The aim of this study was the investigation of the encapsulation of folic acid (FA) in a polymer matrix and of its release behaviour in acidic sweat solution. In the literature, there are more studies on the encapsulation of the vitamin in polymer. To the best of our knowledge, no study in the literature evaluates the in vitro release behaviour and encapsulation of FA in nanofibres for dermal applications. In the present study, unusual electrospun fibres were developed for the release of FA and to overcome the poor release in oral applications, and also the optimum amount of FA added to fibres was determined.

Experimental

Preparation of polymer solutions for electrospinning

Gelatin was dissolved in pure water and acetic acid binary-solvent system (7:3 w/w) solution and stirred for 2 hours at ambient conditions to obtain a 20% (w/w) gelatin solution. PVA powder was also dissolved in pure water at 90 °C till a 10% (w/w) homogeneous PVA solution was obtained. PVP powder was also dissolved in ethanol to obtain a 30% (w/w) PVP solution. At the same time, folic acid was dissolved in 1 M 1 ml $NaHCO_3$ solution for each different amount. Subsequently, different concentrations (19, 22, and 25 mg) of folic acid solutions were added to these polymer solutions separately and mixed in a sealed bottle overnight. The polymer-vitamin mixtures were transferred into a plastic syringe (10 ml) that was attached to a stainless steel nozzle. Pure PVA, gelatin and PVP solutions were also prepared as control (***Figure 1***).

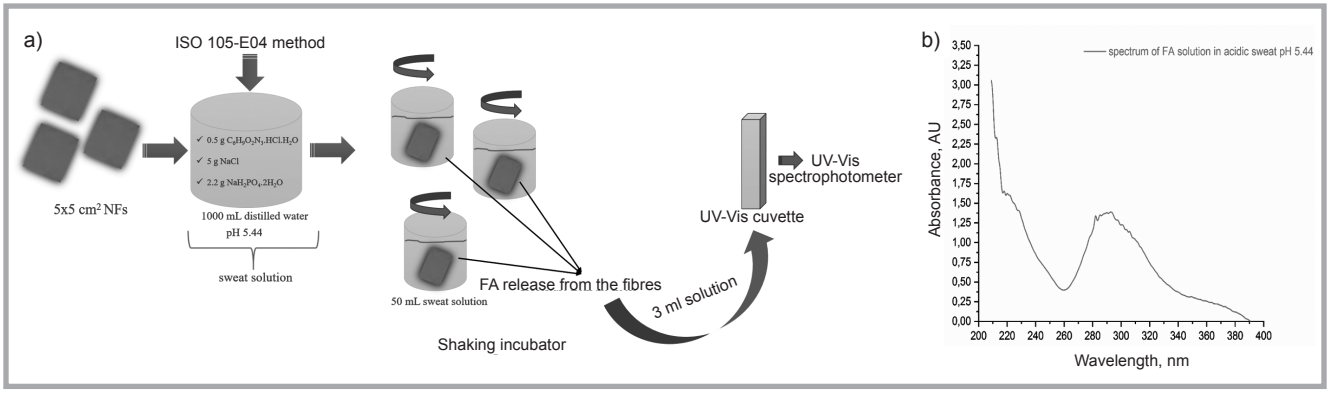

Figure 2. *a) Schematic illustration of release study and b) UV- spectra of FA solution in acidic sweat pH 5.44.*

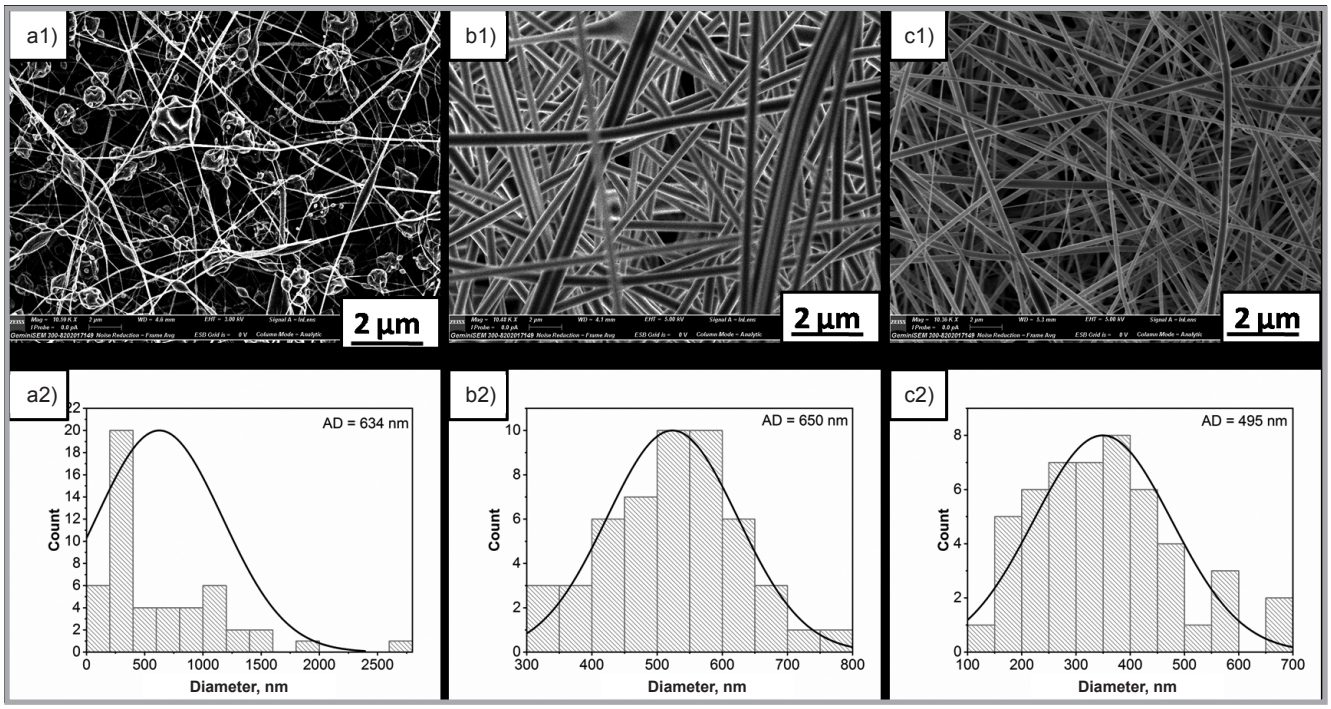

Figure 3. *SEM micrographs and fibre diameter distribution of PVA (a1 & a2), gelatin (b1 & b2) and PVP (c1 & c2) nanofibres.*

Fabrication of nanofibres

The electrospinning device (INOVENSO Nanospinner24, Turkey) consists of an electrical power supply, syringe pump, plastic syringe, and stainless steel nozzle (inner diameter 0.5 mm). The collector consisted of a horizontally positioned board covered with aluminum foil. The PVA/FA, gelatin/FA, and PVP/FA polymer solutions prepared were dispensed through the syringe which was vertical to the collecting plate. The FA-loaded electrospun fibres were fabricated at high voltage.

Characterization

Scanning Electron Microscopy (SEM)

The morphology of all nanofibres was observed with a Carl Zeiss/Gemini 300 Scanning Electron Microscope (SEM) (ZEISS Ltd., Germany). All samples were coated with gold for 20 minutes before analysis. The average fibre diameters were measured using Image J, version 1.520 software.

Thermal analysis (TGA)

TA/SDT650 TGA (USA) was used for thermal analysis. TGA analyses were performed under a nitrogen atmosphere at a 20 °C min^{-1} heating rate, in a 30-600 °C temperature range, and oxygen atmosphere was applied at heating rate of 20 °Cmin^{-1} and temperature of 600-900 °C.

Attenuated Total Reflectance Infrared Spectroscopy (ATR-FTIR)

FTIR data were obtained using a Thermo Nicolet iS50 FTIR (USA) spectrometer with an Attenuated Total Reflectance adapter (ATR) (Pike, USA) in the range of 4000-400 cm^{-1}, recorded with 16 scans at 4 cm^{-1} resolution.

In-vitro **release study**

The pH of the human skin is acidic between 4.2 and 5.6 [38]. Therefore, artificial sweat solutions were prepared using the ISO 105-E04 method. The vitamin release behaviour of 19,22 and 25 mg of FA loaded with PVA, gelatin and PVP nanofibers was studied in the artificial sweat solutions at pH 5.44 by the total immersion method [34, 39]. 3 ml of the solution was taken out at specific time intervals, and the corresponding absorbance value was determined on a UV-Vis spectrophotometer (Scinco/NEOYSY 2000) at λ_{max} = 282 nm, which was the characteristic peak of folic acid.

Regression analysis was carried out to establish an equation for calculation of the concentration from UV-Vis absorbance values. Reference solutions were prepared from folic acid in the laboratory. Firstly, 10 mg of folic acid was dissolved in 200 ml of stock sweat solution. Afterward, this solution was diluted 100 times to prepare five different reference solutions. The absorption value of the reference solutions prepared was measured at 282 nm, and the equation was calculated by analysing the regression relationship (R^2) between absorbance and concentration. A higher R^2 of

Table 2. *Nanofibre samples and their process conditions.*

Fibre type	Voltage, kV	Distance, mm	Flow rate, ml/h	Humidity, %
PVA	27	98	5	<60
PVA19	27	98	5	<60
PVA22	27	98	5	<60
PVA25	27	98	5	<60
Gelatin	25	80	3	<60
Gel19	25	80	3	<60
Gel22	25	80	3	<60
Gel25	25	80	3	<60
PVP	25	88	1	<60
PVP19	25	88	1	<60
PVP22	25	88	1	<60
PVP25	25	88	1	<60

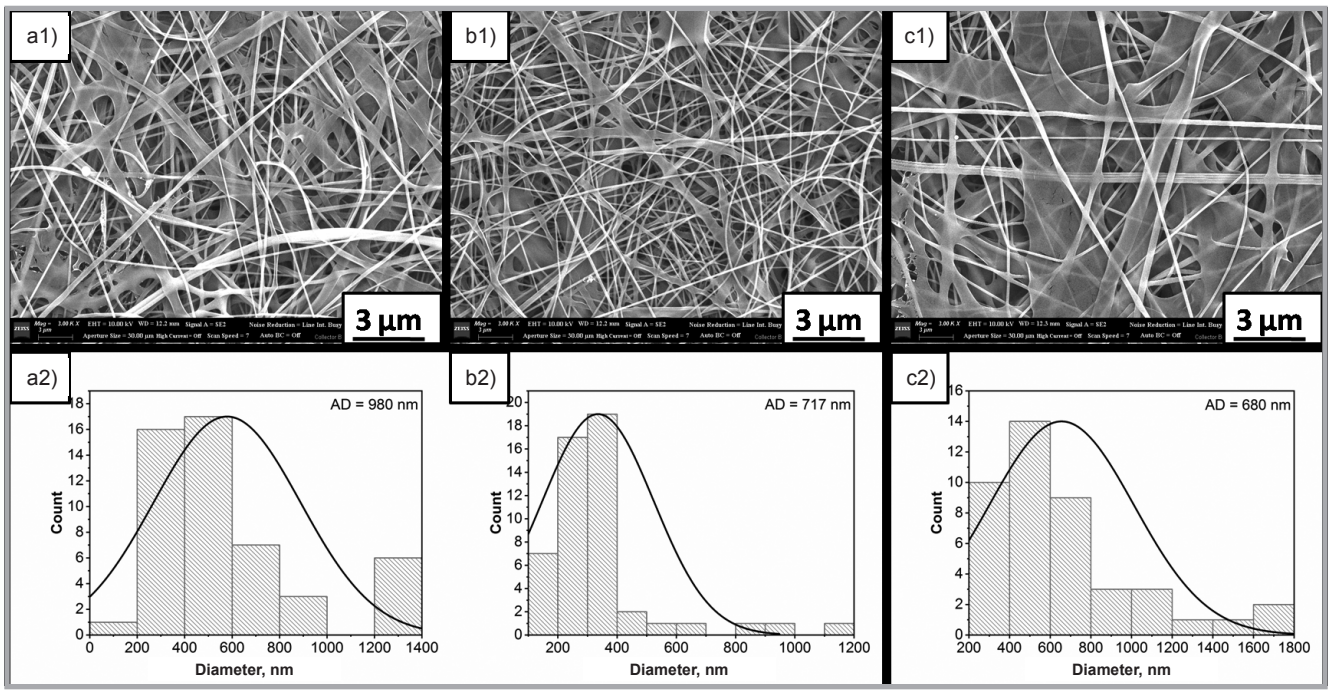

Figure 4. *SEM micrographs and fibre diameter distribution of fibre (a1 & a2) PVA19, (b1 & b2) PVA22, (c1 & c2) and PVA25 electrospun nanofibres.*

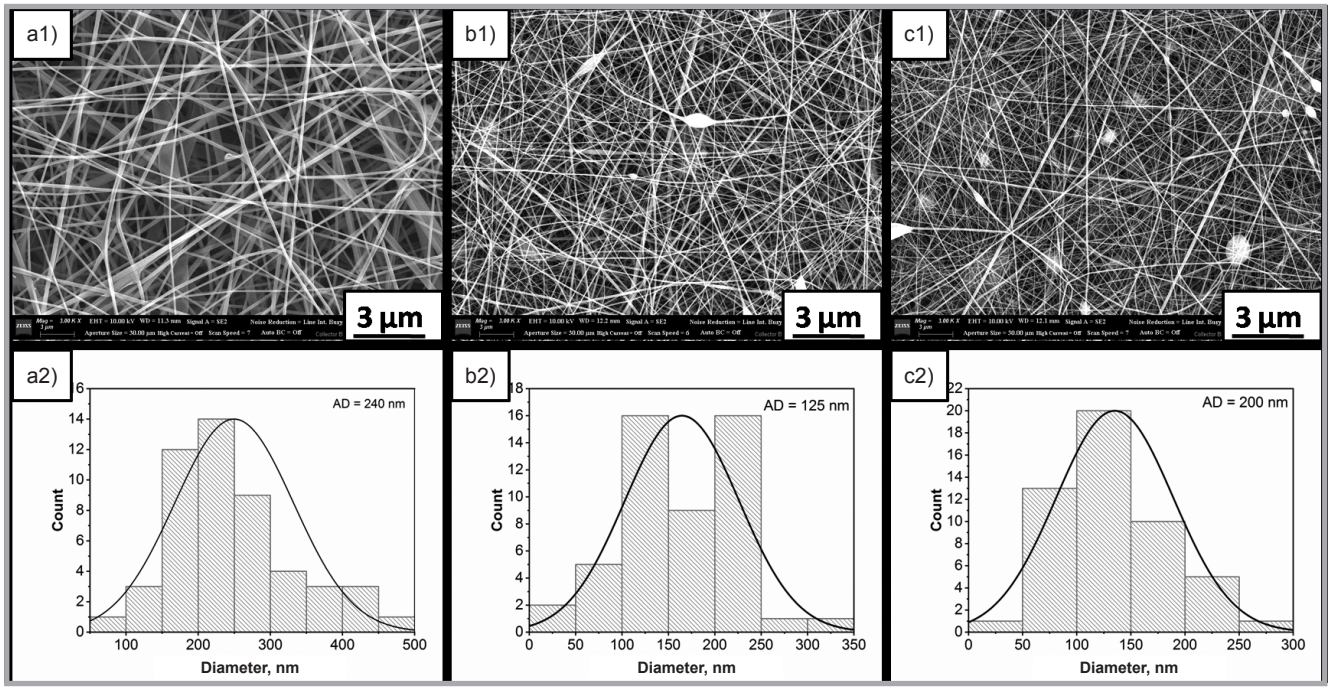

Figure 5. *SEM micrographs and fibre diameter distribution of fibre (a1 & a2) Gel19, (b1 & b2) Gel22, (c1 & c2) and Gel25 gelatin electrospun nanofibres.*

the equation shows the reliability and precision of the method.

The equation was calculated from the following:

$$Y = 0{,}0486X + (-0{,}0402)\ (R^2 = 0{,}99992) \quad (1)$$

where, X is the concentration of FA (mg/l) and Y the solution absorbance at 282 nm (linear range of 0.5-25 mg/l).

Results and discussion

Morphology of electrospun nanofibres

The morphological structure and average fibre diameters of PVA, gelatin and PVP nanofibres are presented in ***Figure 3***, respectively. It was easy to find that the PVA nanofibres had a bead-like structure, the cause of which was the low concentration of PVA solution [40, 41] Unfortunately, in the pretesting of PVA concentration, PVA nanofibres with an increment in PVA viscosity were not obtained. Therefore, the formation of nanobeads on the string structure was inevitable. In addition to this, it was reported that fibre-bead formation occurred with increasing high voltage [42, 43].

The pure PVA nanofibres, which had an unwanted bead-like structure, showed an average fibre diameter of 634 nm, while

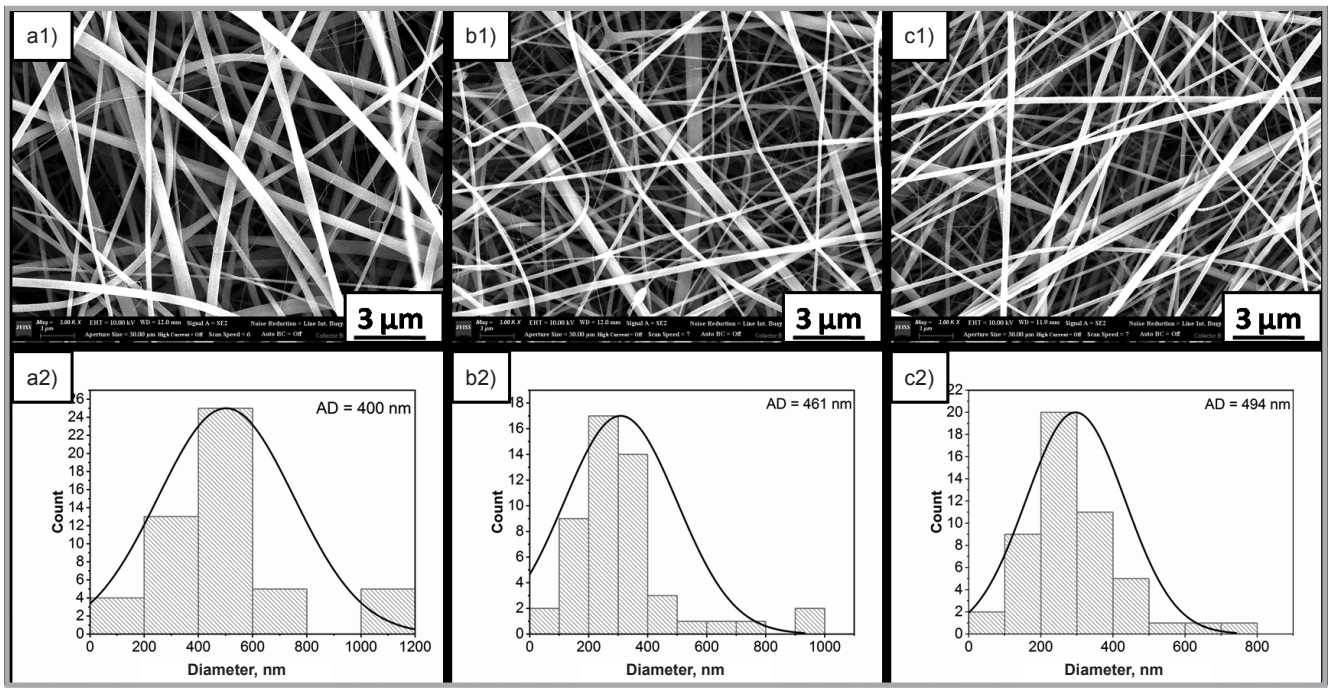

Figure 6. *SEM micrographs and fibre diameter distribution of fibre (a1 & a2) PVP19, (b1 & b2) PVP22, (c1 & c2) and PVP25 electrospun nanofibres.*

the pure gelatin and PVP samples exhibited an average diameter of 650 and 495 nm, respectively (***Figure 3.b2*** *&* ***3.c2***).

The PVA-FA nanofibres reveal a surface with the formation of a heterogeneous web structure. According to ***Figure 4.a***, the thick fibre formation is similar to the two-dimensional ribbon structure existing in PVA nanofibres. When 22 mg of FA was added to PVA solutions, the fibres were transformed into a smoother 3D structure. Micrographs of the 25 mg FA-loaded PVA nanofibres show a broad range fibre diameter and that using excessive amounts of FA destroyed the thin fibre structure. The incorporation of FA to the PVA solutions resulted in a smaller fibre diameter (***Figure 4.a2-4.c2***). The average fibre diameters gradually decreased to 980 nm and 680 nm with an increment in the FA concentration to 19 mg (***Figure 4.a1*** and ***4.a2***), and 25 mg (***Figure 4.c1*** and ***4.c2***), respectively.

When the FA concentration increased from 19 mg to 25 mg, FA-loaded gelatin nanofibres showed a substantially decreased average diameter fibre compared to the pure gelatin sample (***Figure 5.a2 -5.c2***). 19 mg FA-loaded gelatin nanofibres were smoother and had no bead-like structure, while 22 mg FA-loaded gelatin nanofibres had a rough structure with some bead-like morphology. However, it is desirable to have a smaller fibre diameter in order to increase the vitamin loading capacity in drug delivery systems. Therefore, 22 mg FA-loaded gelatin samples have the most ideal fibre of the vitamin-loaded fibres. SEM micrographs of the PVP nanofibres show continuous, long nanofibres with a fibre diameter in the range of 400-500 nm for all FA-loaded PVP nanofibres, as shown in ***Figures 6.a1*** *&* ***6.a2***, ***6.c1*** *&* ***6.c2***), respectively. The neat PVP nanofibres have a dense,

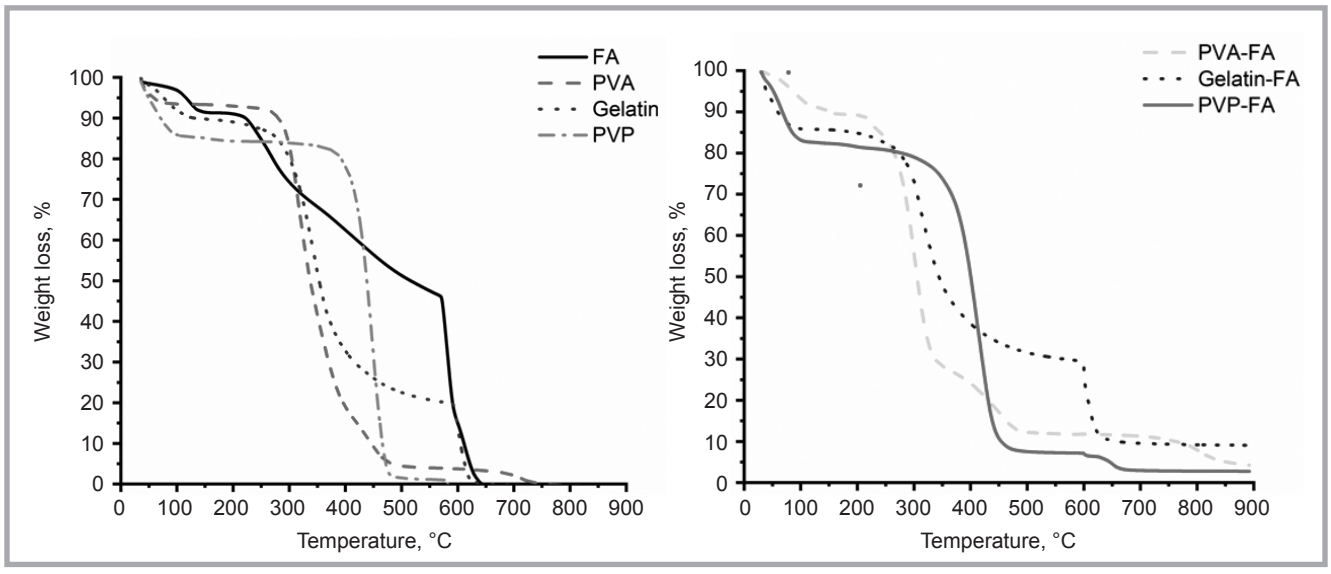

Figure 7. *TGA thermogram of folic acid, pure nanofibres and folic acid (22 mg) loaded nanofibres.*

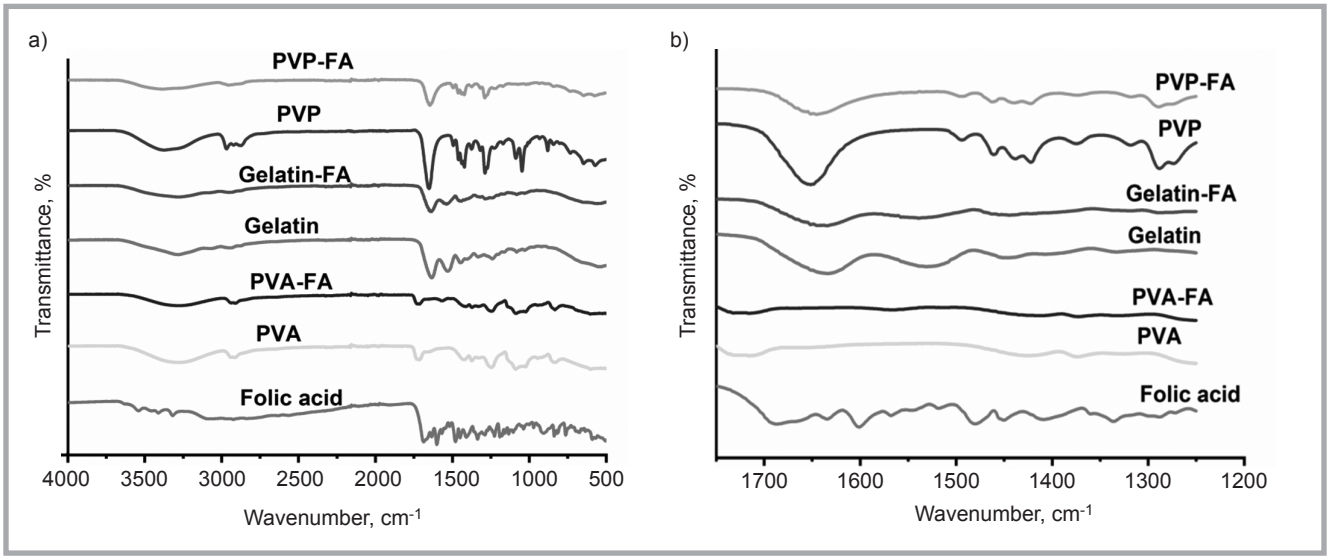

Figure 8. *FTIR-ATR spectra a) and region of interest b) obtained for folic acid, PVA, PVA/FA, gelatin, gelatin/FA, PVP and PVP/FA nanofibres.*

smooth, homogenous and bead-free morphology. According to the fibre distribution, only FA-loaded PVP with nanofibres displayed an increase in the nanofibre diameter. It was explained that each nanofibre group (PVA/FA, gelatin/FA, and PVP/FA) had different process parameters due to the polymer matrix type.

Thermal analysis

Folic acid is a group of heterocyclic compounds based on the 4-[(pteridine-6-ylmethyl)-amino] benzoic acid skeleton conjugated with one or more L-glutamate units [44, 45]. Thermal degradation behaviour is necessary to determine the thermal stability of folic acid. Thermal analysis (TGA) of folic acid was made under a nitrogen atmosphere and interpreted as follows in ***Figure 7***. Vora *et al.* carried out a thermal analysis of folic acid to specify the decomposition temperature [46-49]. It is observed from the curves that folic acid has a mainly four-step decomposition [45]. In the first step in the lower temperature region, between 100-150 °C, weight-loss was occurred due to water evaporation [44, 49]. The second step of weight-loss (170-260 °C) was related to the loss of glutamic acid, then two overlapping reactions began with the loss of pterin and then p-aminobenzoic acid in the remaining two steps [44, 50, 51]. The third weight-loss (240-600 °C) was related to the pyrolysis of the folic acid and the last weight-loss of the folic acid (600-650 °C) to the decomposition of the pyrolyse unit. At a 600 °C temperature, the purge gas was changed from nitrogen to oxygen.

In this study, pure nanofibres were degraded in three steps. The first weight-loss of pure PVA is below 190 °C due to the presence of moisture. The second weight-loss (190-400 °C) was associated with the decomposition of the polymeric side chains in PVA, and the final degradation was related to the breakdown of C-C bonding (the polymer backbone of the main chain of PVA) [52, 53].

For pure gelatin, three thermal degradation steps are observed as reported in the literature [54]. It can be observed that solvent and water evaporation occurred in the range of 25 to 100 °C. Degradation of the fibre started at 250 °C and rapidly continued until 450 °C. In this step, gelatin samples underwent endothermic reactions of hydrolysis and oxidation. The decomposition was complete between 450 to 650 °C, which corresponds to the pyrolysis derived from collagen [55, 56].

The first weight-loss of pure PVP fibres in the temperature range is related to the release of solvent (ethanol) and moisture from fibres. The second weight-loss step started at nearly 400 °C and completely finished at about 550 °C. This step is dependent on the decomposition and pyrolyse of the molecular structure. The last step which barely occurred is related to the decomposition of the pyrolysis structure.

TGA thermograms of the folic acid loaded nanofibres were the same as those for pure nanofibres, apart from the residue part. According to the TGA analysis, folic acid loaded nanofibres gave out residue, with the amount being higher in the case of gelatin than for the others. The residue is related to inorganic sodium bicarbonate. Folic acid dissolved in sodium bicarbonate ($NaHCO_3$) and an inorganic sodium element were integrated into the structure of the fibres.

FTIR analysis

The chemical composition of all nanofibres fabricated and folic acid was confirmed by FTIR spectroscopy. ***Figure 8*** shows that the spectrum of folic acid has many characteristic peaks at 3590, 3496, 3330, 2925, 2840, 1694, 1650, 1605, 1487, and 1405 cm^{-1}. The band between 3600-3200 cm^{-1} is related to the hydroxyl -OH stretching bands of glutamic acid moiety and to the -NH group of the pterin ring. The band at 1650 cm^{-1} belongs to the -C=O bond stretching of $-CONH_2$. The presence of the peak at the 1605 cm^{-1} N-H bending vibration is related the to -CONH group, 1694 cm^{-1} to the -C=O amide stretching of the α-carboxyl group, and 1487 cm^{-1} to the absorption band of the phenyl ring, respectively [50, 56].

Pure PVA nanofibre shows a characteristic peak at 3302 cm^{-1} , identified as -OH stretching, as well as peaks at 2931 cm^{-1}, 2912 cm^{-1} ($-CH_2$ stretching), 1185 and 1091 cm^{-1} (C–O stretching), respectively [53, 57-60].

The characteristic peaks of pure gelatin nanofibre were interpreted as follows: the peak around 3283 cm^{-1} is related to the stretching vibration of N–H (amide II)

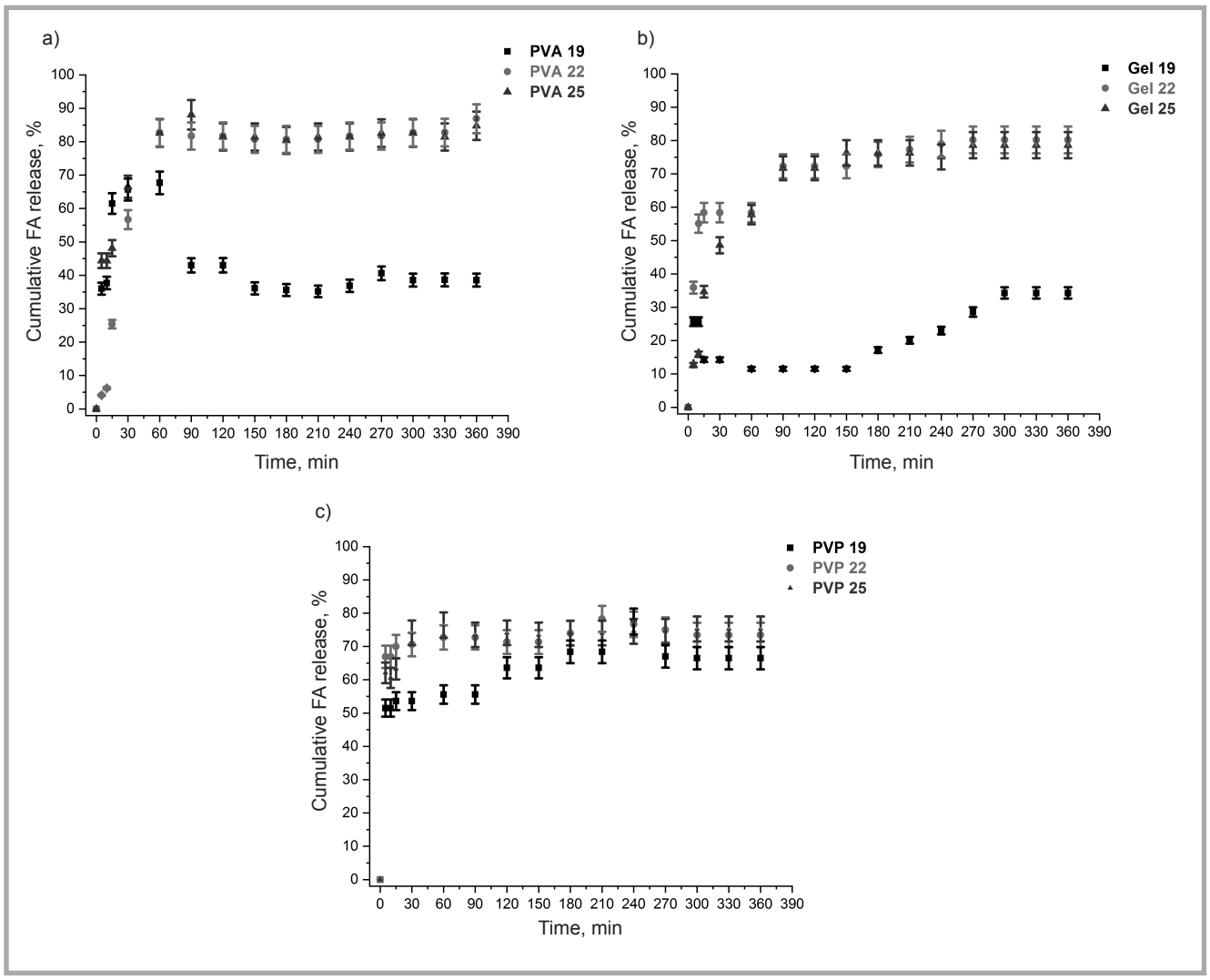

Figure 9. *Release profiles of FA-loaded nanofibres.*

and hydrogen bonding. The broad strong peak at 1640 cm^{-1} corresponds to the stretching vibration of C=O (amide I); that at 1532 cm^{-1} is induced by the bending of N–H (amide II) and stretching of C-N bonds, and the peak at 1245 cm^{-1} is attributed to the bending of N–H [61-63]. The FTIR spectrum of PVP nanofibre has a broad region at 3500-3200 cm^{-1}, which indicates O-H stretching and -CH_2 asymmetric stretching at 2967 cm^{-1}; the most intense and sharp peak at 1656 cm^{-1} is due to the C=O stretching. The four IR multibands around 1450 cm^{-1} (1445, 1438 and 1422 cm^{-1}) were proved to be -CH_2 group peaks. The peaks at 1288 cm^{-1}, 1047 cm^{-1}, and 571 cm^{-1} were assigned to -CN stretching of the amide group, -CH_2 rocking and N-C=O bending, respectively [64-70].

Some differences in the FA-loaded NFs. PVA-FA fibre occurred, with a new peak at 1571 cm^{-1} due to the more intense C=O bond stretching of -$CONH_2$. Also, a new peak was formed at 1142 cm^{-1} due to the C-O-C bond from PVA, and the peaks at 1212 cm^{-1} and 1186 cm^{-1} are related to the characteristic peaks of folic acid. As seen in ***Figure 8***, at 2967 cm^{-1} (-CH_2 bending), 2918 cm^{-1} (C-H stretching), as well as at 1498 and 1375 cm^{-1}, peak intensities decreased in pure PVP fibre. The peaks at 1092 and 1042 cm^{-1} moved away due to -CN stretching of the amide group and -CH_2 rocking, respectively. Moreover, the pyrene ring of PVP was opened at 882 and 844 cm^{-1}. Gelatin-FA nanofibre has a variance of 1600-1400 cm^{-1} .

UV-Vis spectroscopy-release of FA from FA loaded nanofibres *in vitro*

An FA release study of all FA-loaded electrospun fibres was carried out over a period of 8 hours in acidic media at 37.5 °C (***Figure 9***). This period is sufficient for the utilisation of vitamin loaded nanofibres in transdermal applications [23]. Within the first 30 min, 65.7%, 56.68%, and 66.52% for the 19, 22, and 25 mg PVA/FA fibres, respectively, had been released, and after 8 hours 67.7% of FA had been released from the 19 mg PVA/FA fibres, 86.88% from the 22 mg PVA/FA fibres and also 88.07% from the 25 mg PVA/FA fibres. It is seen from the release curve (***Figure 9.a***) that there was an initial burst release within the fibres, which is often due to the far higher amount of the drug on the fibre surface and to the non-homogenous distribution of FA in the fibres. Similarly, hydroquinone-loaded PVA nanofibres showed an initial burst release from the fibres in the first 2 hours [71]. Moreover, Thakkar *et al.* reported a total drug release from antidiabetic repaglinide/PVA fibres of almost 90% for the first 10 min. [72]. The drug release behaviour of nanofibres is due to polymer erosion, diffusion, and a combination of the two [35]. The percentage of FA release until 90 min was not significantly different among the various FA loadings. However, PVA19 showed a re-

duced FA release profile. The smaller and highly porous structure of nanofibres allow drug particles to diffuse out of the polymer matrix more efficiently [73]. Moreover, SEM images (***Figure 4.a1*** & ***4.a2***) confirmed this case, which is due to the higher fibre diameter of PVA19 (980 nm). It is evidenced that PVA22 and PVA25 samples showed good sustainability within the release behavior of the FA from the fibres. This reflects that hydrophilic based PVA nanofibres enhanced the dissolution rate of folic acid substantially. Several factors affect the drug release percentage from drug-loaded fibres like the drug and polymer matrix type (i.e., hydrophilicity and hydrophobicity) and drug-polymer interaction as well [74]. From SEM images it appears that the average fibre diameters of Gel/FA nanofibres were less than those of PVA/FA fibres. Each the electrospun PVA/FA fibres had a much higher FA release compared to all the Gel/FA fibres, the reason for which could also be the interaction (intermolecular hydrogen bonding) between amine groups within the structure of gelatin and pteridine and para-amino-benzoic acid groups within the structure of folic acid. Therefore, fibrous gelatin released small amounts of the vitamin from its structure. The Gel/FA fibres (***Figure 9.b***) at the end of 15 min showed a burst release profile of 14.3%, 58.4%, and 34.7% for the 19, 22, and 25 mg Gel/FA fibres respectively. Then a gradual release was obtained till 240 min for the Gel22, Gel25, and Gel19 samples, with the highest fibre diameter exhibited by FA for a release of 34.3% after 6 hours.

For electrospun PVP/FA fibres, more than 50% of the FA within the fibres was released within the first 5 min., while the entire FA release process finished at a slightly increase after 6 hours. Additionally, the nanofibres indicated a relatively steady behavior after 210 min. A similar FA release behaviour was observed for all fibres. The sustained release of FA from PVP fibres continued for over 60 min. with the drug remaining within the medium. There was no significant change in the percentage of FA release from the fibres when the quantity of FA in PVP fibres was increased from 19 to 25 mg. The *in-vitro* release behaviour of Glibenclamide/PVP nanofibres was found to reach maximum drug release in acidic media within the first 5 min, as a result of which the release process was completed in 480 min. [75]. UV-Vis analysis results revealed that all fibres have a fast releasing behaviour, and when the dry fibres, such as in a face mask, are placed on a sweaty skin surface, vitamin molecules can quickly disintegrate from the fibres and penetrate to the skin.

Conclusions

In this study, folic acid loaded PVA, gelatin, and PVP nanofibres were successfully fabricated via electrospinning, and the structure of the resulting fibres was evaluated by TGA and FTIR analysis. FTIR spectra indicate that peak intensities of the FA-loaded fibres decreased relative to pure fibres. TGA thermograms show that FA-loaded fibres began to degrade earlier than for pure ones due to the vitamin's sensitivity to heat. Moreover, inorganic compounds ($NaHCO_3$) caused residue of about 1.5-2%. The morphology of all vitamin loaded electrospun fibres substantially changes with an increasing folic acid content. The following UV-Vis and SEM analysis proved that the fibre diameter and percentage of vitamin release were directly proportional for each fibre group. However, PVA22 nanofibres have the highest vitamin release value (88.07%) after 8 hours, which is often associated with the polymer type and polymer-vitamin interactions. The percentage of vitamin release also increases due to the increased amount of vitamin loaded into the fibres as well. The *in-vitro* study showed that the initial burst release in acidic media may due to the heterogenous vitamin distribution within the fibre. The utilisation of hydrophilic based fibres within the process also seriously affects the entire vitamin release period. FA-loaded hydrophilic nanofibres can be promising material as fast-dissolving transdermal delivery systems, especially when used as a face mask.

Acknowledgements

This study was supported by Bursa Technical University Scientific Research Projects Coordination Unit (SRP Project No. 190D003). We would like to thank the employees of the Scientific and Technological Research Council of Turkey- Bursa Test and Analysis Laboratory (TUBİTAK-BUTAL) for supporting the preparation of artificial sweat solutions.

References

1. Yılmaz F, Celep G, Tetik G. *Nanofiber Research* 2016; 7, 127-146.
2. Pathak C, Vaidya FU, Pandey SM. *Applications of Targeted Nano Drugs and Delivery Systems*, 2019; 3, 1-33.
3. A. Frenot and I. S. Chronakis, *Curr. Opin. Colloid Interface Sci.* 2003; 8, 64-75.
4. Zuo F, Tan DH, Wang ZS, Jeung WC, Bates M, Bates F S. *ACS Macro Lett.* 2013; 2: 301-305.
5. Brown TD, Dalton PD, Hutmacher DW. Prog. Polym. Sci. 2016; 56: 116-166.
6. Lian H, Meng Z. *Bioactive Materials* 2017; 2, 96-100.
7. Zhou FL, Gong RH. *Polym. Int.,* 2008; 57, 837-845.
8. Ma PX, Zhang RJ. Biomed. Mater. Res. 1999; 46: 60-72.
9. Hartgerink JD, Beniash E, Stupp SI. *Science* 2001; 294:1684-1688.
10. Damien X, Samways SK, Dong H. Bioactive Materials 2017; 2, 260-268.
11. Abdolahi A, Hamzah E, Ibrahim Z, Hashim S. Materials 2012; 5, 1487-1494.
12. Esenturk İ, Erdal M, Gungor S. J. Fac. Pharm. I.U. 2016; 46, 49-69.
13. Sabantina L, Hes L, Mirasol JR, Cordero T, Ehrmann A. Water Vapor Permeability through PAN Nanofiber Mat with Varying Membrane-Like Areas. *FIBRES & TEXTILES in Eastern Europe* 2019; 27, 1(133): 12-15. DOI: 10.5604/01.3001.0012.7502.
14. Yildiz A, Atav R, Aydi M. Production of Polyvinylpyrrolidone Nanowebs Containing Zinc Cyclohexane Mono Carboxylate via Electrospinning and Investigation of Antibacterial Efficiency. *FIBRES & TEXTILES in Eastern Europe* 2019; 27, 6(138): 91-96. DOI: 10.5604/01.3001.0013.4473
15. Yan T, Zhang M, Shi Y, Li Y. Dichloromethane-Extract of Propolis (DEP) and DEP/PLA Electrospun Fiber Membranes. *FIBRES & TEXTILES in Eastern Europe* 2018; 26, 6(132): 57-62. DOI: 10.5604/01.3001.0012.5163.
16. Stratton S, Shelke NB, Hoshino K, Rudraiah S, Kumbar SG. *Bioactive Materials* 2016; 1: 93-108.
17. Wu J, Hong Y. *Bioactive Materials* 2016; 1, 93-108.
18. Waghmare VS, Wadke PR, Dyawanapelly S, Deshpande A, Jain R. *Bioactive Materials* 2018; 3: 255-266.
19. Rather HA, Thakore R, Singh R, Jhala D, Singh S, Vasita R. *Bioactive Materials* 2018; 3: 201-211.
20. Mark R, Langer P, Langer R. *Nat. Biotechnol* 2008; 26: 1261-1268.
21. Rramaswamy R, Mani G, Venkatachalam S, Venkata RY, Lavanya JS, Choi EY. *J. Drug Delivery Sci. Technol.* 2018; 44, 342-348.
22. Shi Y, Wei Z, Zhao H, Liu T, Dong A, Zhang J. *J. Nanosci. Nanotechnol.* 2013; 13: 3855-3863.
23. Fathi-Azarbayjani A, Qun L, Chan Y W, Cha S Y. *AAPS Pharm. Sci. Tech.* 2010; 11: 1164-1170.
24. Sheng X, Fan L, He C, Zhang K, Mo X, Wang H. *Int. J. Biol. Macromol.* 2013; 56: 49-56.

25. Son YJ, Kim WJ, Yoo HS, *Arch. Pharmacal Res.* 2013; 37: 69-78.
26. Kaestli LZ, Wasilewski-Rasca AF, Bonnabry P, Vogt-Ferrier N. *Drugs Aging* 2008; 25, 269-280.
27. Kamble P, Sadarani B, Majumdar A, Bhullar S. *J. Drug Delivery Sci. Technol.* 2017; 41: 124-133.
28. Estevinho BN, Carlan I, Blaga A, Rocha F. *Powder Technol.* 2016; 289: 71-78.
29. Colombo VE, Gerber F. *Food Struct.* 1991; 10: 161-170.
30. Braga D, Chelazzi L, Grepioni F, Maschio L, Nanna S, Taddei P. *Cryst. Growth Des.* 2016; 16: 2218-2224.
31. Uy SJY, Cabrera MJF, Camacho DH. *DLSU Research Congress* 2016; ISSN: 2449-3309.
32. Liang XS, Ma CH, Li PX, Liu XL, Zhao FQ. *Adv. Mater. Res*. 2012; 549: 74-77.
33. Taepaiboon P, Rungsardthong U, Supaphol P. *Eur. J. Pharm. Biopharm.* 2007; 67, 387-397.
34. Madhaiyan K, Sridhar R, Sundarrajan S, Venugopal JR, Ramakrishna S. *Int. J. Pharm.* 2013; 444**,** 70-76.
35. Li H, Wang M, Williams GR, Wu J, Sun X, Lv Y, Zhu LM. *RSC Adv.* 2016; 6: 50267-50277.
36. Fan L, Wang H, Zhang K, Cai Z, He C, Sheng X, Mo X. *RSC Adv.* 2012; 2: 4110.
37. Zarandi MA, Rezaeian I, Motealleh B, Gholami M, Zahedi P, Salehpour A. *IET Nanobiotechnol* 2015; 9: 191-200.
38. Schmid-Wendtner MH, Korting HC. *Skin Pharmacol. Physiol.* 2006; 19, 296-302.
39. Mendes AC, Gorzelanny C, Halter N, Schneider SW, Chronakis IS. *Int. J. Pharm.* 2016; 510: 48-56.
40. Kuo TY, Jhang CF, Lin CM, Hsien TY, Hsieh HJ. *Open Phys.* 2017; 15: 1004-1014.
41. Zhang C, Li Y, Wang P, Zhang H. *Comp. Rev. Food Sci. Food Saf*. 2020; 1-24.
42. Yao ZC, Yuan Q, Ahmad Z, Huang J, Li JS, Chang MW. *Polymers* 2017; 9**,** 265.
43. Lu W, Sun J, Jiang X. *J. Mater. Chem. B.* 2014; 2: 2369.
44. Jankovi B. *AAPS Pharm. Sci. Tech.* 2010; 11: 103-112.
45. Hamed E, Attia MS, Bassiouny K. *Bioinorg. Chem. Appl.* 2009; 1-6.
46. Vora A, Riga A, Dollimore D, Alexander KJ. *Therm. Anal. Calorim.* 2004; 75, 709-717.
47. Vora A, Riga A, Dollimore D, Alexander KJ. *Thermochim. Acta,* 2002; 392-393: 209-220.
48. Vora A, Riga A, Alexander K. *Instrum. Sci. Technol.* 2002; 30: 193-203.
49. Bandara S, Carnegie C, Johnson C, Akindoju F, Williams E, Swaby JM, Oki A, Carson LE. *Heliyon* 2018 4**,** e00737.
50. Yadav V, Rohilla Y, Choudhary M, Choudhary N, Budhwar V. *Int. Res. J. Pharm.* 2018; 9, 6-15.
51. Branton A, Trivedi MK, Trivedi D, Nayak G, Jana S.*J. Nat. Ayurveda Integr. Med.*, 2019 https://doi.org/10.23880/jonam-16000176.
52. Rianjanu A, Kusumaatmaja A, Suyono EA, Triyana K. *Heliyon* 2018; 4, 1-19.
53. HuiLee J, SooLee U, Jeong K, Seo Y, Park S, Kim H. *Polym. Int.* 2010; 59: 1683-1689.
54. Jalaja K, Kumar PRA, Dey T, Kundu SC, James NR. *Carbohydr. Polym.* 2014; 114, 467-475.
55. Salles THC, Lombello C, D'Ávilaa MA. *Mat. Res.* 2015; 18, 509-518.
56. Rujitanaroj P, Pimpha N, Supaphol P. *Polymer* 2008; 49: 4723-4732.
57. Venkatasubbu GD, Ramasamy S, Ramakrishnan V, Janakiraman K. *Adv. Powder Technol.* 2013; 24: 947-954.
58. Kuo TY, Jhang CF, Lin CM, Hsien TY, Hsieh H J. *Open Phys.* 2017; 15: 1004-1014.
59. Sekar AD, Muthukumar H, Chandrasekaran NI, Matheswaran M. *Chemosphere* 2018; 205: 610-617.
60. Kim KO, Akada Y, Kai W, Kim BS, Kim IS. *J. Biomater. Nanobiotechnol.* 2011; 2: 353-360.
61. Kotatha D, Hirata M, Ogino M, Uchida S, Ishikawa M, Furuike T, Tamura HJ. *Nanotechnol.* 2019; 1-11.
62. Ji L, Qiao W, Zhang Y, Wu H, Miao S, Cheng Z, Gong Q, Liang J, Zhu A. *Mater. Sci. Eng. C,* 2017; 78: 362-369.
63. Haider S, Al-Masry WA, Bukhari N, Javid M. *Polym. Eng. Sci*. 2010; 50: 1887-1893.
64. Ke R, Yi W, Tao S, Wen Y, Hongyu Z. *Mater. Sci. Eng. C*, 2017; 78: 324-332.
65. Reksamunandar RP, Edikresnha D, Munir MM, Damayanti S, Khairurrijal S. *Procedia Engineering,* 2017; 170: 19-23.
66. Deniz AE, Vural HA, Ortaç B, Uyar T. *Mater. Lett.,* 2011; 65: 2941-2943.
67. Szilagyi IM, Santala E, Heikkila M, Kemell M, Nikitin T, Khriachtchev L, Rasanen M, Ritala M, Leskela M. *J. Therm. Anal. Calorim.* 2011; 105, 73-81.
68. Bai J, Li Y, Zhang C, Liang X, Yang Q. *Colloids Surf., A,* 2008; 329: 165-168.
69. Sriyanti I, Edikresnha D, Rahma A, Munir MM, Rachmawati H, Khairurrijal K. *Int. J. Nanomed.* 2018; 13: 4927-4941.
70. Edikresnha KD, Sriyanti I, Munir MM, Khairurrijal S. *IOP Conf. Ser. Mater. Sci. Eng.* 2017; 202: 1-7.
71. Fathi-Azarbayjani A, Talebi N, Kambiz Diba. *Int. J. Polym. Anal. Ch.* 2019; 24: 227-235.
72. Thakkar S, More N, Sharma D, Kapusetti G, Kalia K, Misra M. *Drug Dev. Ind. Pharm.* 2019; 45, 1920-1930.
73. Shen X, Xu Q, Xu2 Shi, Li J, Zhang N, Zhang L. *J. Nanosci. Nanotechnol.* 2014; 14: 5258-5265.
74. Aavani F, Khorshidi S, Karkhaneh A. *J. Med. Eng. Technol.* 2019; 43: 38-47.
75. Jain K, Awasthi S, Kumar P, Somashekariah BV, Phani AR. *Middle East J. Sci. Res.* 2014; 22: 1176-1180.

Received 12.04.2020 Reviewed 29.07.2020